Assessment of endocrine disruptor impacts on lipid metabolism in a fatty acid-supplemented HepaRG human hepatic cell line

Kévin Bernal, Charbel Touma, Béatrice Le Grand, Sophie Rose Reyhan Basaran, Selenay Degerli, Valentine Genet, Dominique Lagadic-Gossmann, Xavier Coumoul, Corinne Martin-Chouly, Sophie Langouët, et al.

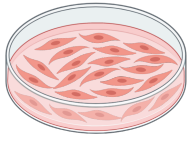

In vitro:
human hepatic
HepaRG cells

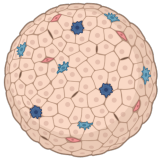

2D model - 5 days

Co-exposure

Endocrine disruptors 10 nM - 25 µM + **Fatty acids** 50 - 200 µM

3D model - 14 days

Gene expression

Protein level

Lipid droplet staining

VLDL export

Cell respiration

Lipid oxidation

Perilipin 2 ↗
(p,p'-DDE and DEHP)

Long-chain fatty acid oxidation ↘
(p,p'-DDE)

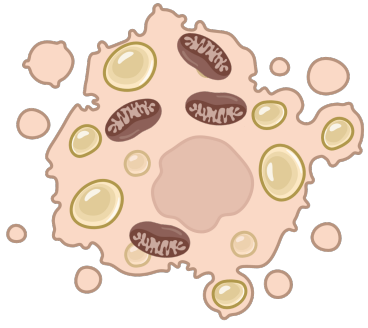

Accumulation of lipid droplets
(p,p'-DDE and phthalates)

Development of an automated detection method specific for lipid droplets to support IATA

Title

Assessment of endocrine disruptor impacts on lipid metabolism in a fatty acid-supplemented HepaRG human hepatic cell line.

Authors

Kévin Bernal[1], Charbel Touma[2], Béatrice Le-Grand[1], Sophie Rose[2], Selenay Degerli[1], Valentine Genêt[2], Dominique Lagadic-Gossmann[2], Xavier Coumoul[1], Corinne Martin-Chouly[2], Sophie Langouët[2], Etienne Blanc[1]

[1] Université Paris Cité, T3S, Inserm UMR-S 1124, 45 rue des Saints Pères, Paris, France.

[2] Inserm, EHESP, Irset (Institut de recherche en santé environnement et travail) – UMR-S 1085, Université de Rennes, France.

Corresponding author

Dr. Etienne Blanc: etienne.blanc@u-paris.fr

Abstract

The incidence of metabolic dysfunction-associated steatotic liver disease (MASLD) is increasing worldwide. This disease encompasses several stages, from steatosis to steatohepatitis and, eventually, to fibrosis and cirrhosis. Exposure to environmental contaminants is one of the risk factors and an increasing amount of evidence points to a role for endocrine disrupting compounds (EDCs). This study assesses the impact of selected EDCs on the formation of lipid droplets, the marker for steatosis in a hepatic model. The mechanisms underlying this effect are then explored. Ten compounds were selected according to their obesogenic properties: bisphenol A, F and S, butyl-paraben, cadmium chloride, p,p'-DDE, DBP, DEHP, PFOA and PFOS. Using a 2D or 3D model, HepaRG cells were exposed to the compounds with or without fatty acid supplementation. Then, the formation of lipid droplets was quantified by an automated fluorescence-based method. The expression of genes and proteins involved in lipid metabolism and the impact on cellular respiration was analyzed. The formation of lipid droplets, which is revealed or enhanced by oleic acid supplementation, was most effectively induced by p,p'-DDE and DEHP. Experiments employing either 2D or 3D culture conditions gave similar results. Both compounds induced the expression of PLIN2. p,p'-DDE also appears to act by decreasing in fatty acid oxidation. Some EDCs were able to induce the formation of lipid droplets, in HepaRG cells, an effect which was increased after supplementation of the cells with oleic acid. A full understanding of the mechanisms of these effects will require further investigation. The novel automated detection method described here may also be useful in the future as a regulatory test for EDC risk assessment.

Keywords

MASLD; Endocrine disruptors; Mechanistic toxicology; Lipid metabolism; HepaRG; Risk assessment

1. Introduction

Over the past decades, metabolic dysfunction-associated steatotic liver disease (MASLD), formerly known as non-alcoholic fatty liver disease (NAFLD), has emerged as the most prevalent liver disease worldwide. It now affects one-quarter to one-third of the general population and the number of cases continues to grow (Le et al. 2022; Riazi et al. 2022; Younossi et al. 2016). MASLD has been defined recently by a multi-society Delphi consensus (Rinella et al. 2023). It covers a broad spectrum of liver outcomes, ranging from steatosis to metabolic dysfunction-associated steatohepatitis (MASH), which can lead to fibrosis, cirrhosis and ultimately to hepatocellular carcinoma (Hardy et al. 2016). MASLD is part of steatotic liver disease (SLD) and encompasses patients who have hepatic steatosis and at least one of the five cardiometabolic risk factors. Steatosis in individuals is defined by an excessive accumulation of fat in >5 % of the hepatocytes. A steatosis without any cardiometabolic risk factors or other specific SLD etiology is defined as cryptogenic SLD. MASLD is associated most often with other disorders such as obesity, type 2 diabetes mellitus (T2DM) and metabolic syndrome (Fan et al. 2017; Yki-Järvinen 2014; Younossi et al. 2019). Affecting several tissues (liver, adipose tissue and the pancreas), MASLD is, thus, a multifactorial disease which is characterized by multiple metabolic dysfunctions as a consequence of the interplay between genetic and environmental factors (Lim et al. 2023). Liver functions are altered by these factors through several mechanisms such as an increase in the content of hepatic triglycerides (TG), mitochondrial alterations, oxidative stress, inflammation and insulin resistance (Fang et al. 2018).

In addition to these risk factors for MASLD, an increasing amount of evidence now indicates that environmental factors and, in particular, endocrine-disrupting compounds (EDCs), are involved in the development of the disease (Foulds et al. 2017; Heindel et al. 2017; Wahlang et al. 2019). Multiple endocrine signaling pathways regulate liver functions and EDCs legitimately impact these functions (Bernal et al. 2022). Some families of chemicals, mainly used as plasticizers, are suspected to induce specific disorders of lipid homeostasis. Among them, bisphenols and phthalates have been found to be associated, in the general US population, with a higher risk of liver steatosis (Cai et al. 2021; Kim et al. 2019). Exposure to EDCs, particularly perfluorinated alkyl substances (PFAS) which may mimic fatty acid signaling with consequent adverse impacts on hepatic lipid metabolism (Sen et al. 2022), can occur also

through contaminated food or water. Despite these observations, few tests for metabolic disruptions have been accepted or are currently under development by the Organization for Economic Cooperation and Development (OECD) or the US Environmental Protection Agency (EPA). This regulation is particularly deficient as to the identification and the risk assessment of chemicals that can induce liver steatosis.

The European OBERON project (https://oberon-4eu.com) has as its goal the development of an integrated testing strategy (ITS) to detect EDC-related metabolic disorders by developing or improving and validating a battery of test systems. It is based on the concept of an integrated approach for testing and assessment (IATA) (Audouze et al. 2020). On the basis of epidemiological studies supported by human biomonitoring data which suggest an association with metabolic disorders, 10 EDCs were selected for study: bisphenol A (BPA), bisphenol F (BPF), bisphenol S (BPS), butylparaben (BP), cadmium chloride ($CdCl_2$), 1,1-dichloro-2,2-bis(4-chlorophenyl)ethene (p,p'-DDE), dibutyl phthalate (DBP), bis(2-ethylhexyl) phthalate (DEHP), perfluorooctanoic acid (PFOA) and perfluorooctanesulfonic acid (PFOS). These chemicals are widely used, in large volumes, and they exhibit potential diabetogenic and obesogenic properties (Heindel et al. 2022).

The present study focuses on the *in vitro* impact of these compounds on lipid metabolism, effects which could lead to liver steatosis. The HepaRG cell line was used as a 2D human liver model and some of the results obtained were confirmed under 3D culture configurations. This cell line, composed of human hepatocytes and cholangiocytes, is a recognized mixed model for the study of both drug effects and intermediary metabolism (Tascher et al. 2019). The Hepoid-HepaRG 3D model exhibits enhanced hepatic differentiation and additional metabolic functions (Rose et al. 2022). As liver steatosis can be induced by multiple environmental factors including lipid overload or exposure to chemicals, we tested the hypothesis as to whether exposure to chemicals could increase the effect of lipid overload on liver cell triglyceride accumulation. To this end, the HepaRG cell line, in both 2D and 3D configurations, was exposed to EDCs along with fatty acid (FA) supplementation. Cellular lipid accumulation was measured, after exposure to the selected compounds, under several culture conditions. A novel technical protocol employing fluorescence microscopy was used to quantify lipid droplets and overall triglyceride content was determined. To decipher putative underlying mechanisms and identify biomarkers of exposure and effect, the expression of several genes and proteins, known to be involved in the development of steatosis, as well as physiological parameters also were analyzed.

2. Materials and methods

2.1 Compounds and cell culture

The different compounds used are listed in **Supplementary Method** (references and suppliers) and EDCs were prepared in 100 % dimethyl sulfoxide (DMSO).

Human HepaRG hepatoma cells were obtained from Dr. Philippe Gripon and were cultured and differentiated as previously described with 1.7 % DMSO to induce differentiation of the cells (Aninat et al. 2006; Gripon et al. 2002; Tascher et al. 2019). Following cell differentiation and five days after seeding, cells were exposed to pollutants, at various concentrations, or to the vehicle with a final concentration of 1.7 % DMSO and for different time periods (cf. **figure legends**). The protocols are presented in **Supplementary Figure 1**. Fatty acid supplementation of cells was performed with several concentrations of oleic acid (OA) or a mixture of palmitic and oleic acid (PA:OA) as explained in **Supplementary Method**. For Hepoid®-HepaRG 3-dimensional (3D) culture, type I collagen was used and diluted in the culture medium as previously described (Rose et al. 2022). The treatment of Hepoid-HepaRG took place 5 days after seeding in collagen, for 14 days in a DMSO-free medium in the presence of 5 % fetal bovine serum.

2.2 Cell viability

In order to evaluate viability after EDC exposure in the 2D cell model, differentiated HepaRG cells were seeded into 96-well plates at a density of 8×10^4 cells per well prior to exposure to each compound, alone or in combination with FA, at concentrations varying from 100 nM to 25 µM during 3, 5 or 14 days. At the end of exposure, cell viability was assessed with a microplate reader (Spark®, Tecan) using 3 dyes: resazurin, 5-carboxyfluorescein diacetate acetoxymethyl ester (CFDA-AM) and neutral red, as previously described (Raska et al. 2018). For the Hepoid® 3D model, cell viability was assessed by measuring ATP content using the CellTiter-Glo® 3D Assay (Promega) according to the manufacturer's protocol. Luminescence was measured after 30 min of incubation using the PerkinElmer Enspire 2300 multilabel reader.

2.3 Lipid droplet assessment

Lipid droplet quantification was performed using epifluorescence microscopy by staining lipid droplets and cell nuclei with Nile Red (1 µM, 510/573 nm to assess only triglycerides) and Hoechst 33342 (1 µg/mL, 350/461 nm), respectively. Differentiated HepaRG cells were seeded

into 96-well plates at a density of 8×10^4 cells per well. Images were obtained and analyzed using an ImageXpress Pico (Molecular Devices). A macro was programmed to select only the lipid droplets in the cells based on cell size and intensity exceeding the background. To compare the impact of the different treatments, a steatosis index was defined (**Supplementary Figure 2**). The results are expressed as a percentage (%) based on the mean steatosis index of the control according to the exposure procedure.

In Hepoid-HepaRG, lipid droplets were measured after fixation with 4 % paraformaldehyde containing 5 % sucrose for 10 min at room temperature. Hoechst 33342 and LipidTOX™ HCS (ThermoFisher, 1/1000) staining were performed simultaneously to stain nuclei and lipid droplets, respectively. Images were acquired with a Leica SP8 confocal microscope with a 40x oil objective. Images (40 µm stack) were then analyzed using ImageJ software using a specific macro that detects lipid droplets and nuclei. The results are expressed as the number of lipid droplets *per* cell.

2.4 Triglyceride content

Hepoid-HepaRG were treated for 14 days at a concentration of 10 µM p,p'-DDE with and without supplementation, consisting of a mixture of palmitic and oleic acid (50 µM each). The medium was renewed every 48 hours. Triglyceride concentration was measured using the Triglyceride-Glo Assay (Promega) according to the manufacturer's protocol. The luminescence measurement was performed using the PerkinElmer Enspire 2300 multilabel reader. Results, proportional to the amount of glycerol in the sample, were then normalized to cell viability as estimated by ATP measurement.

2.5 Gene expression quantification and immunoblotting

For gene expression analysis, total RNAs were extracted using the GenElute™ Mammalian Total RNA Miniprep kit (#RTN350, Sigma-Aldrich). Reverse transcription was performed using the high-capacity cDNA reverse transcription Kit (#4368814, Applied Biosystems®) following the manufacturer's instructions on 1 µg of RNA in 50 µL. Then, quantitative PCR was performed using 20 ng of cDNA per reaction using CFX 384 thermocycler (Bio-Rad®). with Takyon SYBR® 2X qPCR Mastermix Blue (Eurogentec®) with 0.3 µM of each primer (**Supplementary Table S1**). The relative mRNA level was estimated with the delta-delta C_t method using *RPL13A* and *HPRT* as reference genes (Livak and Schmittgen 2001).

For immunoblotting, cells were scraped into RIPA buffer (#R0278, Sigma-Aldrich). Total proteins (7.5 µg) were separated by SDS-PAGE (Mini-PROTEAN TGX gels, #4561086, Biorad) and transferred onto a PVDF membrane (Transblot turbo, #1704156, Biorad). The membrane was saturated for 1 h at room temperature with a blocking buffer (#927-60001, LI-COR Biosciences) diluted in PBS/0.2 % TWEEN (v:v) and then overnight at 4°C with the primary antibody diluted in saturation buffer (references and the conditions in **Supplementary Table S2**). After the final washes, the intensities of the bands were quantified using an Odyssey infrared Imager (LI-COR Biosciences).

2.6 Apolipoprotein B (ApoB) quantification

ApoB secretion was quantified using the human apolipoprotein B ELISA PRO kit, as described by the manufacturer (#3715-1HP, Mabtech). Briefly, differentiated HepaRG were seeded in 96 well plates and treated with the different exposure protocols. Three days after the last treatment, the supernatant was collected and frozen at -20°C until quantification. Absorbance at 450 nm was measured (background at 600 nm) with a microplate reader (Enspire 2300, PerkinElmer). The concentration of ApoB was then extrapolated using a five-parameter logistic curve fit (GraphPad Prism, 9.5.1 version). The results were then normalized to the total amount of proteins.

2.7 Measurement of oxidative respiration by Seahorse technology

The oxygen consumption rate (OCR) and the extracellular acidification rate (ECAR) were measured using a Seahorse XFe24 Analyzer (Agilent) to determine key parameters involved in mitochondrial metabolism. After seeding into Seahorse 24 well-plates (#100777-004; Agilent) at a density of 1.5 x 10^5 cells *per* well, differentiated HepaRG cells underwent different exposure scenarios. The Mitostress protocol was performed, as described by the manufacturer. At last, Hoechst 33342 (1 µg/mL final) was injected and incubated for 15 min to stain the nuclei, which were counted by fluorescence microscopy analysis. The results were normalized to the number of nuclei in each well.

To determine the part of the OCR relative to long-chain fatty acid oxidation (LCFAO), cells were cultivated under the same conditions as described previously. After exposure, they were washed twice and incubated for 1 h at 37°C in a CO_2 free atmosphere with DMEM XF medium pH 7.4 supplemented with 2 mM L-glutamine. Three measurements were performed before and after injection of etomoxir (5 µM), an inhibitor of CPT1A. Hoechst 33342 (1 µg/mL) was then

injected, and the cells were incubated for 15 min to stain the nuclei. The respiration relative to LCFAO corresponds to the difference in OCR between the basal respiration and the respiration after etomoxir injection. The results were normalized to the number of cells in each well.

2.8 Statistical analysis

The results are expressed as the mean ± SEM of at least three independent experiments. The number of replicates is given in the figure legends. Statistical analysis and graphing were carried out using GraphPad Prism (10.0.2 version). A Shapiro-Wilk normality test was performed to evaluate the Gaussian distribution of each dataset. In the case of a normal distribution, data were analyzed by one-way or two-way ANOVA followed by a Dunnett (all conditions compared to control) or Bonferroni (all conditions compared to their respective control) post hoc test to assess differences between specific conditions. For datasets that did not follow a normal distribution, data were analyzed using Kruskal-Wallis test followed by a Dunn's correction. A p-value was used to determine sample significance with *, $p < 0.05$; **, $p < 0.01$; ***, $p < 0.001$ and ****, $p < 0.0001$.

3. Results

The compounds used in this study were selected for their obesogenic capacities based on epidemiological studies which focused on quantitative measurements of adipogenesis, body mass index or waist circumference (Audouze et al. 2020). Complementary experimental studies based on robust cell line models of adipogenesis were also used. For example, accumulation of lipids was observed in mouse 3T3-L1 differentiated adipocytes after exposure to several common or analog compounds: 25 µM PFOS or PFOA (in the presence of rosiglitazone), 20 µM BPA, BP or mono(2-ethylhexyl) phthalate (MEHP) – a metabolite of DEHP – and 10-30 µM p,p'-DDE (Mangum et al. 2015; Modaresi et al. 2022; Taxvig et al. 2012). On the basis of those results, a dose of 25 µM was, thus, selected as an upper limit and, subsequently, used in this study.

3.1 Assessment of the cytotoxicity of the selected EDCs

When evaluating steatosis development in HepaRG cells, viability assays were performed using various concentrations (from 100 nM to the upper limit of 25 µM) to be sure that the compounds were used at sub-toxic concentrations. None of the compounds exhibited any toxicity on the HepaRG cells in 2D culture after 72 h or 14 days (**Supplementary Table 3A**), except for 10 µM cadmium which seemed to alter lysosome integrity as early as 72 h.

The viability of Hepoid-HepaRG was assessed after exposure of the spheroids for 72 hours and 14 days to the various EDCs, at concentrations between 100 nM to 25 µM. No toxic effect was detected irrespective of the concentration used (even at concentrations as high as 25 µM), except for $CdCl_2$ which decreased the cellular ATP content at both 10 and 25 µM beginning at 72 hours (**Supplementary Table 3B**).

As EDCs were tested with additional exposures, such as to fatty acid supplementation (OA 100 µM or PA:OA 50 µM each), the cytotoxicity under these conditions also was assessed (**Supplementary Figure 3**). After 5 days, no effect was observed, which was coherent with the results obtained at 72 h and 14 d, except for 25 µM DEHP which non-specifically increased the dehydrogenase activities (**Supplementary Figures 3A-C; Table 3A**).

3.2 Lipid droplet accumulation

Based on the preceding results, we used a concentration of 25 µM for all compounds except for $CdCl_2$ (1 µM) in a first attempt to identify whether the selected EDCs could induce steatosis in

HepaRG 2D model. As stated above, since liver steatosis is often a consequence of a high energy diet, cells were supplemented with OA (100 µM or 200 µM) during exposure to EDCs. An exposure time of 5 days was chosen as a reference for our study, based on previous experiments (Paramitha et al. 2021).

Lipid droplet formation was quantified using fluorescence microscopy images. To compare treatments a specific parameter, the 'steatosis index', was defined (**Supplementary Figure 2**). Without any supplementation, an increase of the steatosis index was observed only following an exposure to 25 µM DEHP, whereas exposure to $CdCl_2$ and PFOS produced a decrease, although not statistically significant (**Figure 1A**). The quantification of total TG content also showed an increase, although non-significant, only after DEHP exposure (**Supplementary Figure 4A**). In comparison, an increase in the steatosis index was observed after exposure to 25 µM of DBP (~2x), p,p'-DDE (~4x) and DEHP (~6x) supplemented with 100 µM OA (**Figure 1B**). Both the density and the size of the lipid droplets were increased (**Figure 1C**). However, no increase in total TG content was observed (**Supplementary Figure 4A**). The effect of p,p'-DDE, DBP and DEHP was less following supplementation with 200 µM OA as compared to 100 µM OA, probably due to the excessive amount of lipid already present in the cells, mitigating the potential (**Supplementary Figure 4B**).

Dose response curves for p,p'-DDE and DEHP, which were the most effective in inducing steatosis following OA supplementation, were then performed. No effect on the steatosis index was observed with increasing concentrations of p,p'-DDE under normal conditions of culture (**Figure 2A**). However, with 100 µM OA supplementation, the steatosis index increased with increasing amounts of p,p'-DDE (significant beginning at a concentration of 10 µM, **Figure 2A**). In contrast, for DEHP, there was an increase in the steatosis index either with or without supplemental OA (**Figure 2B**).

Supplementation with OA increased the effects of exposure to both p,p'-DDE and DEHP by about 40-fold, whereas the supplementation with OA alone increased the steatosis index only 12-fold (**Figure 2C**). These results could reflect a synergistic effect, or at least more than an additive effect, of the combination OA and pollutants.

To approach a more physiological ratio of free fatty acids observed in healthy fasting humans, supplementation with a mixture of OA and PA (50 µM each) also was used (Kokotou et al. 2022). The effects of the pollutants, although similar, were less and were statistically significant only with DEHP (**Supplementary Figure 4C**). Of note, the formation of lipid droplets in the

control cells exposed to fatty acids was lower after the supplementation with the mixture 50:50 µM PA:OA as opposed to that with 100 µM OA alone.

Because steatosis is a reversible process, the capacity of the EDCs to maintain this pathophysiological state also was assessed (**Supplementary Figure 1C**). The release of lipids was observed in the control, for which the steatosis index reverts almost to the level of the control without any supplementation (2.6 % steatosis remaining) (**Supplementary Figure 4D**). This release was statistically significantly decreased following exposure to DEHP (7.4 % steatosis remaining).

In order to estimate the capability of pollutants to affect lipid metabolism in the 3D human hepatic spheroid culture, we analyzed the impact on droplet formation of 4 prototypical representatives of the different EDC families by measuring the lipids in 3D cultures. Hepoid-HepaRG cells were treated with 10 µM BPA, p,p'-DDE, DEHP or PFOA for 14 days. An accumulation of lipid droplets in Hepoid-HepaRG was observed after 14 days of treatment with all 4 compounds tested with a statistically significant increase of 7.6-fold after exposure to p,p'-DDE as compared to the control (**Figure 3A**). A 6.3-fold increase was observed after exposure to DEHP (p=0.08). In this model, our findings also demonstrated that both the mixtures of PA:OA or OA alone similarly increased TG content after 14 days (data not shown). Based on these results, the accumulation of TG following exposure to 10 µM p,p'-DDE with and without supplemental exposure to a FA mixture (PA:OA 50 µM each) was measured. Both p,p'-DDE and FA alone caused a 2-fold increase in cellular TG content as compared to the control. The combination of p,p'-DDE plus FA led to a statistically significant 3.7-fold increase in TG accumulation (**Figure 3B**).

3.3 Impact on lipid metabolism

The increase in lipid droplets could be explained by several mechanisms: increase of the *de novo* FA synthesis, decrease of lipid catabolism, increase of triglyceride and droplet formation, increase of lipid uptake, or decrease of VLDL export. The expression of representative anabolic genes of these pathways was measured by RT-qPCR in 2D HepaRG cells treated with either p,p'-DDE, DBP or DEHP alone or with FA supplementations (**Figure 4**). Details of the qRT-PCR results for each gene are given in the **Supplementary Figures 5-9**.

Whatever the supplementation (no fatty acid or 100 µM OA), exposure to p,p'-DDE decreased the expression of *SREBP1C*, *FASN* and *SCD1*, but did not affect *ACC1* expression. This effect was not observed with PA:OA supplementation. The co-exposure of cells to DBP and FA increased the expression of *SREBP1C*. The expression of the aforementioned genes were unaffected upon exposure of cells to DEHP under any condition.

For the genes involved in TG synthesis, no significant effect of pollutants was observed. Supplementations with FA alone decreased *DGAT2* expression. On the contrary, *PLIN2* mRNA expression increased with the 100 µM OA supplementation (1.5-fold). Co-exposure of cells to both p,p'-DDE and FA led to further increases in *PLIN2* mRNA expression (2.4-fold and 1.7-fold, respectively, with OA and PA:OA). An increase in the amount of PLIN2 protein was observed following exposure of cells to p,p'-DDE or DEHP along with only 100 µM OA (**Figure 5A**).

No major effect on *FATP2* and *CD36* gene expression was observed under any culture condition. Furthermore, no effect was observed on the level of cellular CD36 protein after EDC exposures (**Figure 5B**). On the contrary, exposure to p,p'-DDE (no supplementation) decreased the expression of *FABP1*. FA supplementation also decreased significantly basal *FABP1* mRNA expression, which was not modified by p,p'-DDE but was suppressed by the phthalates in the presence of 100 µM OA and which was alleviated by these pollutants in the presence of 50 µM PA:OA.

A significant decrease of *MTTP* expression was observed in the presence of FA supplementations. However, no effect was observed for *APOB* expression or for APOB secretion, which suggests that these pollutants did not significantly impact VLDL export (**Figure 6A**).

No significant effect upon *CYP4A11* and *CPT1A* gene or protein expression was observed following the different exposures (**Figure 5A**). Cell respiration is coupled with the activity of the Krebs cycle which is fueled by acetyl-coA anabolism the β-oxidation of which provides a significant contribution. Therefore, we measured cell respiration and showed that the basal and maximal respirations were slightly decreased (although non-significantly) by p,p'-DDE either in the presence of absence of additional FA (**Figure 6B-C**). To determine whether this decrease was related to a disruption in lipid oxidation, we measured the long-chain fatty acid oxidation (LCFAO). The LCFAO was reduced by p,p'-DDE (0.15 pmol/min/1000 cells) as compared to

355 the control (0.46 pmol/min/1000 cells), whereas no impact on this parameter was observed with
356 DEHP (0.51 pmol/min/1000 cells) (**Figure 6D**).

4. Discussion

In the present work, we show that exposure to some EDCs along with FA promote liver steatosis development. In the human hepatic cell line, HepaRG, among the 10 compounds studied, exposure to DEHP increased the formation of lipid droplets in both the 2D and 3D models. Furthermore, using a FA supplementation which mimics a dietary intake, the exposure to two phthalates (DBP and DEHP) or one organochloride pesticide (p,p'-DDE) exacerbated the formation of droplets after 5 days in the 2D HepaRG model.

Under normal culture conditions, only DEHP induced the formation of lipid droplets. This effect was observed previously with the HepaRG model, after 7 days of exposure to a lower concentration of DEHP, 10 nM (Franco et al. 2020). However, the 2D cell culture in that study was performed in collagen-coated plates and the DMSO was reduced to 0.6 % for the duration of exposure. Under those conditions, the cells might be more sensitive, since BPA (10 nM) and PFOA (100 nM) also induced lipid droplet formation. Other studies have reported an increase in TG content in HepaRG cells after BPA, PFOA or PFOS exposure, however these studies used longer times of exposure (3 weeks of BPA, also during the proliferation phase) or higher concentrations of EDCs (greater than 50 µM of PFOS and 200 µM of PFOA) (Bucher et al. 2017; Louisse et al. 2020). These results were confirmed in a 3D Hepoid-HepaRG model, in which an increase in lipid droplets was observed after 14 days of treatment with 10 µM BPA, p,p'-DDE, DEHP, or PFOA. Of note, in the study by Franco and collaborators mentioned above, PFOS decreased the total lipid content (but not neutral lipid content) (Franco et al. 2020). Under our conditions, without FA supplementation, neutral lipid content was decreased by PFOS. Together, these results highlight i) the fact that the effects of PFAS on MASLD are still unclear and might depend on multiple parameters (diet, hepato-toxic compounds…), as suggested by a recent meta-analysis of rodent and human studies (Costello et al. 2022) ; ii) the fact that the culture conditions in different studies may affect the results obtained with the same pollutant, which suggesting that studies of the exposome which integrate these multiple parameters should be carried out to better understand the effect of pollutants in the context of a diverse hepatic vulnerability. Moreover, when considering whole organisms, the intricate relationships and dialogue between organs could also lead to different effects. Indeed, it has been shown recently in zebrafish larvae that p,p'-DDE but not DEHP significantly increases steatosis (Le Mentec et al. 2023). In line with this observation, differences among species should also be better characterized.

A major finding of the present study is the capacity for some EDCs to induce steatosis in a dose-dependent manner when supplemented with fatty acids (**Figure 2**), whereas few (DEHP) or no effects (DBP and p,p'-DDE) were observed with the pollutant exposure alone. Thus, the supplementation with fatty acids appears to reveal steatotic properties of compounds, probably in a synergistic manner. This is in line with the "multiple-hit" theory likely involving environmental pollutants (Byrne and Targher 2015; Wahlang et al. 2019). This has been observed in several studies in which animals were fed a high fat diet (HFD) and exposed to DEHP (rat), p,p'-DDE (rat) or other types of pollutants such as TCDD (mice) (Duval et al. 2017; Rodríguez-Alcalá et al. 2015; Zhang et al. 2023). However, this synergistic effect is not always observed. For instance, it has been shown that a combination of HFD and a high dose of p,p'-DDE (2 mg/kg) in mice leads to a decrease in the amount of lipid in liver and in triglyceride content (Howell et al. 2015). The "synergistic" effect of fatty acid supplementation and pollutant exposure needs to be evaluated further. Studies on different species, different doses and times of exposure, carefully defined protocols and mathematical modelling (Ma and Motsinger-Reif 2019) need to be combined to elucidate the mechanisms involved (common or distinct.

Several protocols of FA supplementation were employed in the present study. The choice of 100 µM OA was made with respect to the amounts measured in fasting individuals. The serum used to supplement the cell cultures already contains TG (58 mg/dL) and probably free FA. Thus, the supplementation used in the present study might be compared to a transient overload of FA after a meal. Indeed, when OA was removed, the cellular lipid droplets disappeared rapidly and completely. Since we observed an increase in lipid accumulation after co-exposure to EDCs and FA which persisted after withdrawal of the OA, it can be assumed that cyclic intake of FA would lead to a gradual increase in cellular lipid droplets, which would eventually reach a steatotic steady state.

With the same total concentration of free fatty acids in the medium, fewer droplets were observed following supplementation with PA:OA as compared to OA alone. PA has been shown to be a poor inducer of lipid droplets in the HepG2 model (Eynaudi et al. 2021). In our study, under PA:OA supplementation, the difference in the steatosis index after EDC exposure appeared to be less marked as compared to OA (100 µM) supplementation. The pollutants seem,

thus, to act on processes involving OA. In the Hepoid-HepaRG 3D model, the PA:OA supplementation was used, since it more accurately reflects human exposure to a combination of fatty acids on a daily basis (ranging from 0.2 to 5 mmol/L), rather than focusing solely on OA (Abdelmagid et al. 2015; Staiger et al. 2004). Under these conditions, the effect of exposure to p,p'-DDE appeared in the PA:OA supplemented Hepoid-HepaRG 3D cell culture model whereas no effect was observed in the 2D model.

In this study, the increased cellular accumulation of neutral lipids is associated with an increase of PLIN2 expression following co-exposure of cells to p,p'-DDE or DEHP and OA. To our knowledge, this is the first time that this effect has been observed in a human model after exposure to p,p'-DDE. This is coherent with the recently characterized effect of p,p'-DDE on plin2 expression in zebrafish larvae (Le Mentec 2023). In mice, an increase in hepatic *Plin2* gene expression has been observed previously following exposure to DEHP (Li et al. 2020). This protein is a major component of the membrane of lipid droplets and plays a crucial role in their formation and stabilization. In *Plin2* null mice, the *Plin2* deficiency led to reduced hepatic TG content and prevented the induction of steatosis when mice were fed a Western-diet (Libby et al. 2016; Mardani et al. 2019). Conversely, overexpression of Plin2 in murine hepatocyte AML12 cells (derived from liver of transgenic mice overexpressing transforming growth factor-α) reduces the rate of TG loss by suppressing autophagy in the hepatocytes (Tsai et al. 2017). These studies support the idea that the increase in PLIN2 observed upon exposure to p,p'-DDE or DEHP allows the maintenance of a higher level of lipid droplets in cells and helps to explain their accumulation in the present model.

The increase in PLIN2 expression cannot entirely explain the increase of lipid droplets observed after exposure of cells to pollutants found in the present study. Despite the variety of possible mechanisms investigated, none of them were sufficient to explain the accumulation of lipid droplets that developed after exposure to DEHP. In HepG2 cells, similar effects were observed although with much higher concentrations of DEHP (100 µM) and OA (500 µM) (Zhang et al. 2017). The mechanism was proposed to be related to oxidative stress and to increased levels of PPARα and SREBP proteins. No change in the expression of the target genes of PPARα (*CPT1A*, *CYP4A11*) or SREBP (*FAS*, *ACC1*, *SCD1*) after DEHP exposure were observed in the present study. However, DBP, another phthalate studied, has the ability to upregulate *SREBP1C* expression under cellular co-exposure with FA. This might explain, partially, the formation of new cellular lipid droplets but may also suggest that different phthalates may have different

impacts. Analysis of the level of oxidative stress in HepaRG after exposure to DEHP as has been performed in several other models such as Hep3B cells or in rats (Chen et al. 2013; Ha et al. 2016) might provide useful insights. *In vivo*, in the context of a HFD, DEHP (0,1 mg/kg/day for 25 weeks) enhanced steatosis in the liver of obese mice which was proposed to be linked to an increase in the expression of *Cd36* (Hsu et al. 2021).

Our preliminary experiments have demonstrated that exposure of cells to p,p'-DDE may impact mitochondrial lipid oxidation (**Figure 6D**). Very few studies deal with the effect of p,p'-DDE on lipid metabolism in hepatic cells. In the human HepG2 cell line, a decrease of basal respiration by p,p'-DDE (10 ng/mL for 24 h) has been shown (Liu et al. 2017). In rodents, exposure to p,p'-DDE has given contradictory results probably related to the use of different protocols. On the one hand, studies have shown a decrease in lipid production or an increase of carnitine palmitoyl-transferase activity and β-oxidation consistent with a role for oxidative stress after exposure to p,p'-DDE for 4 weeks in rats (10 mg/kg) and in mice (2 mg/kg) (Howell et al. 2015; Migliaccio et al. 2019). On the other hand, an enhanced lipogenesis along with an increase of fatty acid, *de novo* synthesis proteins (Acc, Fas and Scd1) has been observed after exposure to p,p'-DDE (8 weeks, 1 mg/kg/day everyday) (Liu et al. 2017; Morales-Prieto et al. 2018). In zebrafish larvae, this effect on lipogenesis has been found to be associated with an upregulation of scd1, involved, in part, in the induction of steatosis (Le Mentec et al. 2023). In the current study, the expression of *SCD1* was decreased, suggesting that the formation of TG might involve mainly saturated fatty acids. In fact, the cellular lipid droplet accumulation could be linked to a decrease in lipid oxidation: indeed, a decreased expression of *FASN* (**Figure 4**) was observed which could lead to the accumulation of malonyl-CoA, an inhibitor of CPT1A.

Based on the European legislation concerning the characterization of EDC, three criteria are required to consider a substance as an EDC: the presence of an adverse outcome, an endocrine mode of action, and a link between these two elements (Andersson et al. 2018). To assess these parameters, the evaluator needs reliable tools and assays. Currently, only 5 *in vitro* methods have been validated by the OECD and 2 by the US-EPA (OECD 2018). It is therefore necessary to provide validated methods as stated recently (Grignard et al. 2022). The method for lipid droplet quantification that we describe in this paper is easy to implement, cheap, and can be used in a relatively high throughput process. Moreover, a list of reference compounds for testing human steatosis endpoints, *in vitro*, has been recently established and our results, obtained with BPA, PFOA, p,p'-DDE, DEHP and OA, fit with those described for TG accumulation

(Kubickova and Jacobs 2023). Thus, we believe that our method could be part of an integrated testing strategy (ITS) to identify metabolic or endocrine disruptors, in particular in line with the adverse outcome pathways (AOP) under development related to steatosis (AOP 34, 36, 57, 58, 59, 60, 62, 232 and 318 from aopwiki.org).

In conclusion, the present study assesses the impact of EDCs on steatosis induction in a 2D HepaRG cell model. Our data suggest that co-exposure with oleic acid, at a physiological concentration, enhances the steatosis-inducing effects of DEHP and reveals a similar impact for p,p'-DDE, and DBP, albeit to a lesser extent. This steatotic effect was confirmed for p,p'-DDE and DEHP in a 3D HepaRG model without any FA supplementation. The molecular mechanisms involved in the accumulation of neutral lipids after pollutant exposure are likely diverse and not fully elucidated. Finally, the method described here for the detection, characterization and quantification of lipid droplets could be useful as an ITS (Integrated Testing Strategy) or an IATA (Integrated Approaches to Testing and Assessment) for EDC risk assessment related to MASLD, or even SLD, to fill gaps in regulatory strategy to support chemical safety.

Acknowledgments

This project is supported by OBERON, a collaborative project funded by the EU Framework Programme for Research and Innovation Action, Horizon 2020, under grant agreement n°825712. This project funded Kévin Bernal's and Charbel Touma's PhD studies, Antoine Legrand's salary (technical support) as well as experimental materials.

Project investigators are hired by the CNRS (DLG), INSERM (SL), Université Paris Cité (BLG, EB, XC) and the Université de Rennes (CMC, SR, VG). The authors would like to thank Dr Martine Aggerbeck and Dr Lawrence Aggerbeck for critical reading of the manuscript. The authors acknowledge the CYTO2BM core facility of BioMedTech Facilities, INSERM US36 | CNRS UAR2009 | Université Paris Cité for assistance with qPCR and SeaHorse analyses.

The graphical abstract was created with BioRender.com.

References

Abdelmagid SA, Clarke SE, Nielsen DE, Badawi A, El-Sohemy A, Mutch DM, et al. Comprehensive Profiling of Plasma Fatty Acid Concentrations in Young Healthy Canadian Adults. PLoS One. 2015 Feb 12;10(2):e0116195.

Andersson N, Arena M, Auteri D, Barmaz S, Grignard E, Kienzler A, et al. Guidance for the identification of endocrine disruptors in the context of Regulations (EU) No 528/2012 and (EC) No 1107/2009. EFSA Journal. 2018;16(6):e05311.

Aninat C, Piton A, Glaise D, Le Charpentier T, Langouët S, Morel F, et al. Expression of cytochromes P450, conjugating enzymes and nuclear receptors in human hepatoma HepaRG cells. Drug Metab Dispos. 2006 Jan;34(1):75–83.

Audouze K, Sarigiannis D, Alonso-Magdalena P, Brochot C, Casas M, Vrijheid M, et al. Integrative Strategy of Testing Systems for Identification of Endocrine Disruptors Inducing Metabolic Disorders—An Introduction to the OBERON Project. Int J Mol Sci. 2020 Apr 23;21(8):2988.

Bernal K, Touma C, Erradhouani C, Boronat-Belda T, Gaillard L, Al Kassir S, et al. Combinatorial pathway disruption is a powerful approach to delineate metabolic impacts of endocrine disruptors. FEBS Lett. 2022 Dec;596(24):3107–23.

Bucher S, Jalili P, Le Guillou D, Begriche K, Rondel K, Martinais S, et al. Bisphenol a induces steatosis in HepaRG cells using a model of perinatal exposure. Environmental Toxicology. 2017;32(3):1024–36.

Byrne CD, Targher G. NAFLD: A multisystem disease. Journal of Hepatology. 2015 Apr 1;62(1, Supplement):S47–64.

Cai S, Fan J, Ye J, Rao X, Li Y. Phthalates exposure is associated with non-alcoholic fatty liver disease among US adults. Ecotoxicology and Environmental Safety. 2021 Nov 1;224:112665.

Chen X, Qin Q, Zhang W, Zhang Y, Zheng H, Liu C, et al. Activation of the PI3K–AKT–mTOR signaling pathway promotes DEHP-induced Hep3B cell proliferation. Food and Chemical Toxicology. 2013 Sep 1;59:325–33.

Costello E, Rock S, Stratakis N, Eckel SP, Walker DI, Valvi D, et al. Exposure to per- and Polyfluoroalkyl Substances and Markers of Liver Injury: A Systematic Review and Meta-Analysis. Environ Health Perspect. 2022 Apr 27;130(4):046001.

Duval C, Teixeira-Clerc F, Leblanc AF, Touch S, Emond C, Guerre-Millo M, et al. Chronic Exposure to Low Doses of Dioxin Promotes Liver Fibrosis Development in the C57BL/6J Diet-Induced Obesity Mouse Model. Environ Health Perspect. 2017 Mar;125(3):428–36.

Eynaudi A, Díaz-Castro F, Bórquez JC, Bravo-Sagua R, Parra V, Troncoso R. Differential Effects of Oleic and Palmitic Acids on Lipid Droplet-Mitochondria Interaction in the Hepatic Cell Line HepG2. Front Nutr. 2021 Nov 12;8:775382.

Fan J-G, Kim S-U, Wong VW-S. New trends on obesity and NAFLD in Asia. Journal of Hepatology. 2017 Oct 1;67(4):862–73.

559 Fang Y-L, Chen H, Wang C-L, Liang L. Pathogenesis of non-alcoholic fatty liver disease in
560 children and adolescence: From "two hit theory" to "multiple hit model." World J
561 Gastroenterol. 2018 Jul 21;24(27):2974–83.

562 Foulds CE, Treviño LS, York B, Walker CL. Endocrine-disrupting chemicals and fatty liver
563 disease. Nat Rev Endocrinol. 2017 Aug;13(8):445–57.

564 Franco ME, Fernandez-Luna MT, Ramirez AJ, Lavado R. Metabolomic-based assessment
565 reveals dysregulation of lipid profiles in human liver cells exposed to environmental obesogens.
566 Toxicology and Applied Pharmacology. 2020 Jul 1;398:115009.

567 Grignard E, de Jesus K, Hubert P. Regulatory Testing for Endocrine Disruptors; Need for
568 Validated Methods and Integrated Approaches. Front Toxicol. 2022 Jan 19;3:821736.

569 Gripon P, Rumin S, Urban S, Le Seyec J, Glaise D, Cannie I, et al. Infection of a human
570 hepatoma cell line by hepatitis B virus. Proc Natl Acad Sci U S A. 2002 Nov 26;99(24):15655–
571 60.

572 Ha M, Wei L, Guan X, Li L, Liu C. p53-dependent apoptosis contributes to di-(2-ethylhexyl)
573 phthalate-induced hepatotoxicity. Environmental Pollution. 2016 Jan 1;208:416–25.

574 Hardy T, Oakley F, Anstee QM, Day CP. Nonalcoholic Fatty Liver Disease: Pathogenesis and
575 Disease Spectrum. Annu Rev Pathol. 2016 May 23;11:451–96.

576 Heindel JJ, Blumberg B, Cave M, Machtinger R, Mantovani A, Mendez MA, et al. Metabolism
577 Disrupting Chemicals and Metabolic Disorders. Reprod Toxicol. 2017 Mar;68:3–33.

578 Heindel JJ, Howard S, Agay-Shay K, Arrebola JP, Audouze K, Babin PJ, et al. Obesity II:
579 Establishing causal links between chemical exposures and obesity. Biochemical Pharmacology.
580 2022 May 1;199:115015.

581 Howell GE, Mulligan C, Meek E, Chambers JE. Effect of chronic p,p′-
582 dichlorodiphenyldichloroethylene (DDE) exposure on high fat diet-induced alterations in
583 glucose and lipid metabolism in male C57BL/6H mice. Toxicology. 2015 Feb 3;328:112–22.

584 Hsu J-W, Nien C-Y, Chen H-W, Tsai F-Y, Yeh S-C, Kao Y-H, et al. Di(2-ethylhexyl)phthalate
585 exposure exacerbates metabolic disorders in diet-induced obese mice. Food and Chemical
586 Toxicology. 2021 Oct 1;156:112439.

587 Kim D, Yoo ER, Li AA, Cholankeril G, Tighe SP, Kim W, et al. Elevated urinary bisphenol A
588 levels are associated with non-alcoholic fatty liver disease among adults in the United States.
589 Liver International. 2019;39(7):1335–42.

590 Kokotou MG, Mantzourani C, Batsika CS, Mountanea OG, Eleftheriadou I, Kosta O, et al.
591 Lipidomics Analysis of Free Fatty Acids in Human Plasma of Healthy and Diabetic Subjects
592 by Liquid Chromatography-High Resolution Mass Spectrometry (LC-HRMS). Biomedicines.
593 Multidisciplinary Digital Publishing Institute; 2022 May;10(5):1189.

594 Kubickova B, Jacobs MN. Development of a reference and proficiency chemical list for human
595 steatosis endpoints in vitro. Front Endocrinol (Lausanne). 2023 Apr 24;14:1126880.

Le Mentec H, Monniez E, Legrand A, Monvoisin C, Lagadic-Gossmann D, Podechard N. A New In Vivo Zebrafish Bioassay Evaluating Liver Steatosis Identifies DDE as a Steatogenic Endocrine Disruptor, Partly through SCD1 Regulation. Int J Mol Sci. 2023 Feb 15;24(4):3942.

Le MH, Yeo YH, Li X, Li J, Zou B, Wu Y, et al. 2019 Global NAFLD Prevalence: A Systematic Review and Meta-analysis. Clinical Gastroenterology and Hepatology. 2022 Dec 1;20(12):2809-2817.e28.

Li Y, Zhang Q, Fang J, Ma N, Geng X, Xu M, et al. Hepatotoxicity study of combined exposure of DEHP and ethanol: A comprehensive analysis of transcriptomics and metabolomics. Food and Chemical Toxicology. 2020 Jul 1;141:111370.

Libby AE, Bales E, Orlicky DJ, McManaman JL. Perilipin-2 Deletion Impairs Hepatic Lipid Accumulation by Interfering with Sterol Regulatory Element-binding Protein (SREBP) Activation and Altering the Hepatic Lipidome. J Biol Chem. 2016 Nov 11;291(46):24231–46.

Lim GEH, Tang A, Ng CH, Chin YH, Lim WH, Tan DJH, et al. An Observational Data Meta-analysis on the Differences in Prevalence and Risk Factors Between MAFLD vs NAFLD. Clinical Gastroenterology and Hepatology. 2023 Mar 1;21(3):619–29.

Liu Q, Wang Q, Xu C, Shao W, Zhang C, Liu H, et al. Organochloride pesticides impaired mitochondrial function in hepatocytes and aggravated disorders of fatty acid metabolism. Sci Rep. Nature Publishing Group; 2017 Apr 11;7(1):46339.

Livak KJ, Schmittgen TD. Analysis of Relative Gene Expression Data Using Real-Time Quantitative PCR and the 2−ΔΔCT Method. Methods. 2001 Dec 1;25(4):402–8.

Louisse J, Rijkers D, Stoopen G, Janssen A, Staats M, Hoogenboom R, et al. Perfluorooctanoic acid (PFOA), perfluorooctane sulfonic acid (PFOS), and perfluorononanoic acid (PFNA) increase triglyceride levels and decrease cholesterogenic gene expression in human HepaRG liver cells. Arch Toxicol. 2020;94(9):3137–55.

Ma J, Motsinger-Reif A. Current Methods for Quantifying Drug Synergism. Proteom Bioinform. 2019 Jul;1(2):43–8.

Mangum LH, Howell GE, Chambers JE. Exposure to p,p′-DDE enhances differentiation of 3T3-L1 preadipocytes in a model of sub-optimal differentiation. Toxicol Lett. 2015 Oct 14;238(2):65–71.

Mardani I, Tomas Dalen K, Drevinge C, Miljanovic A, Ståhlman M, Klevstig M, et al. Plin2-deficiency reduces lipophagy and results in increased lipid accumulation in the heart. Sci Rep. 2019 May 6;9:6909.

Migliaccio V, Scudiero R, Sica R, Lionetti L, Putti R. Oxidative stress and mitochondrial uncoupling protein 2 expression in hepatic steatosis induced by exposure to xenobiotic DDE and high fat diet in male Wistar rats. PLoS One. 2019 Apr 25;14(4):e0215955.

Modaresi SMS, Wei W, Marques E, DaSilva NA, Slitt AL. Per- and polyfluoroalkyl substances (PFAS) augment adipogenesis and shift the proteome in murine 3T3-L1 adipocytes. Toxicology. 2022 Jan 15;465:153044.

Morales-Prieto N, Ruiz-Laguna J, Sheehan D, Abril N. Transcriptome signatures of p,p´-DDE-induced liver damage in Mus spretus mice. Environmental Pollution. 2018 Jul 1;238:150–67.

OECD. Revised Guidance Document 150 on Standardised Test Guidelines for Evaluating Chemicals for Endocrine Disruption, OECD Series on Testing and Assessment, n° 150, Éditions OCDE, Paris. 2018.

Paramitha PN, Zakaria R, Maryani A, Kusaka Y, Andriana BB, Hashimoto K, et al. Raman Study on Lipid Droplets in Hepatic Cells Co-Cultured with Fatty Acids. Int J Mol Sci. 2021 Jul 9;22(14):7378.

Raska J, Ctverackova L, Dydowiczova A, Sovadinova I, Blaha L, Babica P. Tumor-promoting cyanotoxin microcystin-LR does not induce procarcinogenic events in adult human liver stem cells. Toxicology and Applied Pharmacology. 2018 Apr 15;345:103–13.

Riazi K, Azhari H, Charette JH, Underwood FE, King JA, Afshar EE, et al. The prevalence and incidence of NAFLD worldwide: a systematic review and meta-analysis. The Lancet Gastroenterology & Hepatology. 2022 Sep 1;7(9):851–61.

Rinella ME, Lazarus JV, Ratziu V, Francque SM, Sanyal AJ, Kanwal F, et al. A multi-society Delphi consensus statement on new fatty liver disease nomenclature. Hepatology. 2023 Dec;78(6):1966-86.

Rodríguez-Alcalá LM, Sá C, Pimentel LL, Pestana D, Teixeira D, Faria A, et al. Endocrine Disruptor DDE Associated with a High-Fat Diet Enhances the Impairment of Liver Fatty Acid Composition in Rats. J. Agric. Food Chem. American Chemical Society; 2015 Oct 28;63(42):9341–8.

Rose S, Cuvellier M, Ezan F, Carteret J, Bruyère A, Legagneux V, et al. DMSO-free highly differentiated HepaRG spheroids for chronic toxicity, liver functions and genotoxicity studies. Arch Toxicol. 2022 Jan 1;96(1):243–58.

Sen P, Qadri S, Luukkonen PK, Ragnarsdottir O, McGlinchey A, Jäntti S, et al. Exposure to environmental contaminants is associated with altered hepatic lipid metabolism in non-alcoholic fatty liver disease. Journal of Hepatology. 2022 Feb 1;76(2):283–93.

Staiger H, Staiger K, Stefan N, Wahl HG, Machicao F, Kellerer M, et al. Palmitate-Induced Interleukin-6 Expression in Human Coronary Artery Endothelial Cells. Diabetes. 2004 Dec 1;53(12):3209–16.

Tascher G, Burban A, Camus S, Plumel M, Chanon S, Le Guevel R, et al. In-Depth Proteome Analysis Highlights HepaRG Cells as a Versatile Cell System Surrogate for Primary Human Hepatocytes. Cells. 2019 Feb 21;8(2):192.

Taxvig C, Dreisig K, Boberg J, Nellemann C, Schelde AB, Pedersen D, et al. Differential effects of environmental chemicals and food contaminants on adipogenesis, biomarker release and PPARγ activation. Molecular and Cellular Endocrinology. 2012 Sep 25;361(1):106–15.

Tsai T-H, Chen E, Li L, Saha P, Lee H-J, Huang L-S, et al. The constitutive lipid droplet protein PLIN2 regulates autophagy in liver. Autophagy. 2017 May 26;13(7):1130–44.

672 Wahlang B, Jin J, Beier JI, Hardesty JE, Daly EF, Schnegelberger RD, et al. Mechanisms of
673 Environmental Contributions to Fatty Liver Disease. Curr Environ Health Rep. 2019
674 Sep;6(3):80–94.

675 Yki-Järvinen H. Non-alcoholic fatty liver disease as a cause and a consequence of metabolic
676 syndrome. The Lancet Diabetes & Endocrinology. 2014 Nov 1;2(11):901–10.

677 Younossi ZM, Golabi P, de Avila L, Paik JM, Srishord M, Fukui N, et al. The global
678 epidemiology of NAFLD and NASH in patients with type 2 diabetes: A systematic review and
679 meta-analysis. Journal of Hepatology. 2019 Oct 1;71(4):793–801.

680 Younossi ZM, Koenig AB, Abdelatif D, Fazel Y, Henry L, Wymer M. Global epidemiology of
681 nonalcoholic fatty liver disease—Meta-analytic assessment of prevalence, incidence, and
682 outcomes. Hepatology. 2016;64(1):73–84.

683 Zhang W, Shen X-Y, Zhang W-W, Chen H, Xu W-P, Wei W. The effects of di 2-ethyl hexyl
684 phthalate (DEHP) on cellular lipid accumulation in HepG2 cells and its potential mechanisms
685 in the molecular level. Toxicology Mechanisms and Methods. Taylor & Francis; 2017 May
686 4;27(4):245–52.

687 Zhang Y, Feng H, Tian A, Zhang C, Song F, Zeng T, et al. Long-term exposure to low-dose
688 Di(2-ethylhexyl) phthalate aggravated high fat diet-induced obesity in female mice.
689 Ecotoxicology and Environmental Safety. 2023 Mar 15;253:114679.

690

Figures

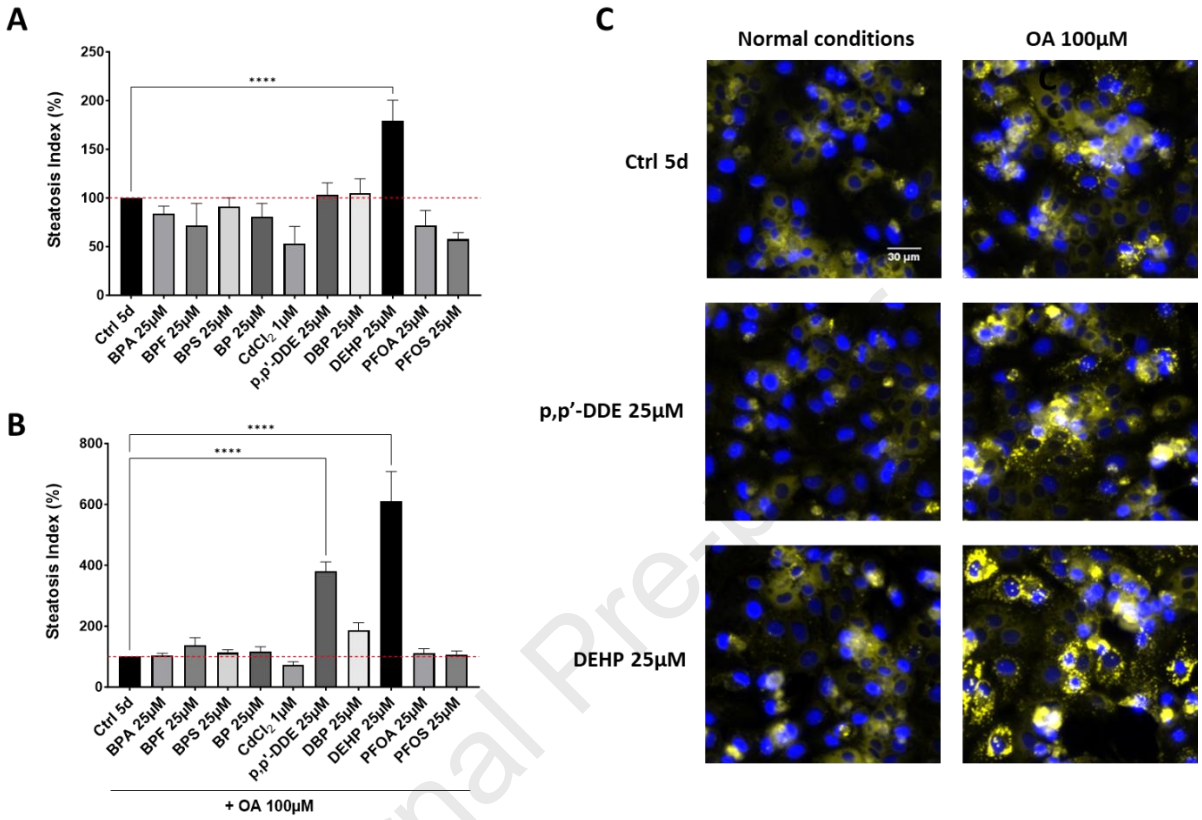

Figure 1: Assessment of steatosis index by fluorescence microscopy in 2D HepaRG cells following exposure to EDCs. Lipid accumulation was evaluated after 5 days of exposure to EDCs (**A**) in HepaRG under normal culture conditions or (**B**) under co-exposure with 100µM oleic acid (OA). To assess triglyceride accumulation, a steatosis index (cf. **Supplementary Figure 2**) was used based on Nile Red staining and analysis with an automated fluorescence microscope. Values are the mean ± SEM relative to control (in %) from at least 4 (**A**) or 5 (**B**) independent experiments in triplicate. Statistical analysis was performed using one-way ANOVA followed by a Dunnett post-hoc correction. ****, $p < 0.0001$. (**C**) Representative fluorescence microscopy images of HepaRG cells after 5 days of exposure with pollutants alone or in combination with 100 µM OA. Cells were stained for nuclei (blue) and neutral lipids (yellow). The images were obtained at 10X magnification. Scale bar is 30 µm.

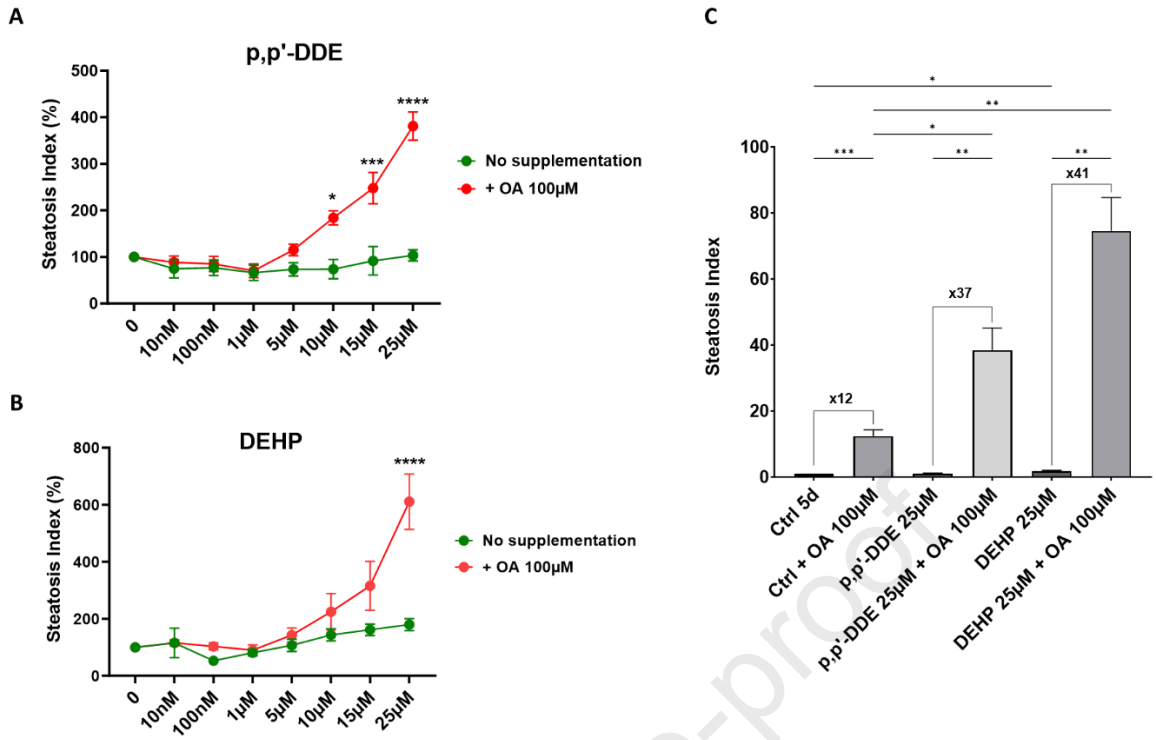

Figure 2: Impact of p,p'-DDE and DEHP exposure on steatosis in 2D HepaRG cells. Assessment by fluorescence microscopy of triglyceride accumulation in HepaRG cells following exposure to different concentrations (10 nM – 25 µM) of (**A**) p,p-DDE alone (green) or in combination with 100 µM oleic acid (OA) (red); (**B**) DEHP alone (green) or with 100 µM OA supplementation (red). Lipid accumulation was evaluated after 5 days of exposure using a steatosis index (cf. **Supplementary Figure 2**) based on Nile Red staining and analysis with an automated fluorescence microscope. (**C**) Steatosis index in HepaRG cells relative to the control following exposure to EDCs alone or in combination with 100 µM OA. The values represent the average steatosis induction factor between the same condition with and without OA supplementation. Values are the mean ± SEM relative to the control (in %) from at least 3 (**A, B**) or 7 (**C**) independent experiments in triplicate. Statistical analysis was performed using one-way ANOVA followed by a Dunnett (**A, B**) or Bonferroni (**C**) post-hoc correction. Stars (**A**, **B**) represent a significant difference between exposure without supplementation and exposure with 100 µM OA supplementation. *, $p < 0.05$; **, $p < 0.01$; ***, $p < 0.001$; ****, $p < 0.0001$.

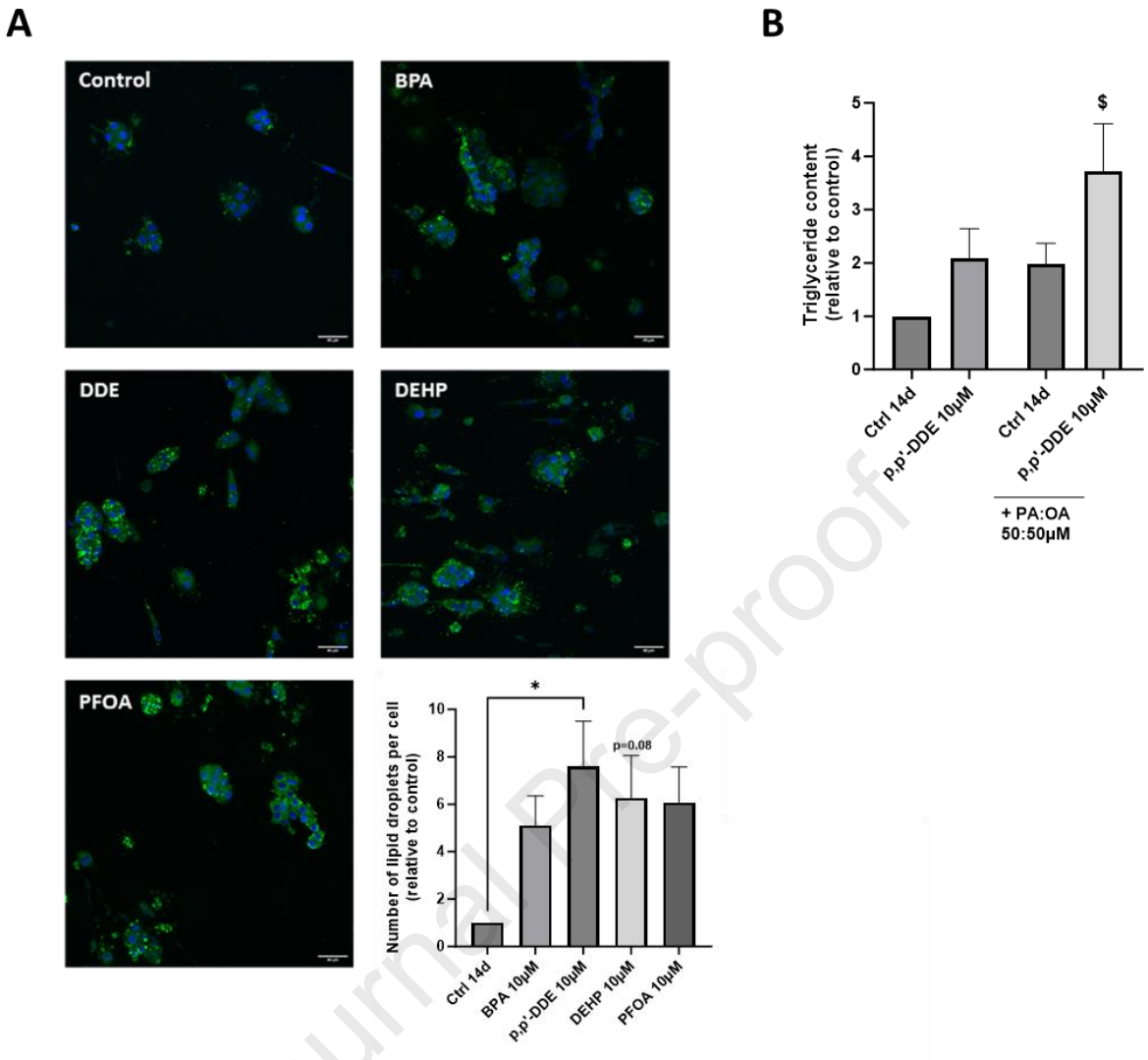

Figure 3: EDC effects on lipid metabolism in Hepoid-HepaRG. (**A**) Representative fluorescence microscopy pictures of Hepoid-HepaRG cells after 14 days of treatment with pollutants alone. Cells were stained for nuclei (blue) and neutral lipids (green). The images were obtained at 40X magnification. Scale bar is 40 µm. The graph shows the quantification of lipid droplets, using a specific macro, relative to control cells. (**B**) Assessment of triglyceride accumulation in Hepoid-HepaRG after 14 days of treatment with p,p'-DDE at 10 µM without or with supplementation with fatty acids (PA:OA, 50:50 µM). All values are the mean ± SEM; n = 3. Statistical analysis was performed using one-way ANOVA followed by a Dunnett (**A**) or Bonferroni (**B**) post-hoc correction. *, $p < 0.05$; $, $p < 0.05$ compared to the control at 14 days without supplementation.

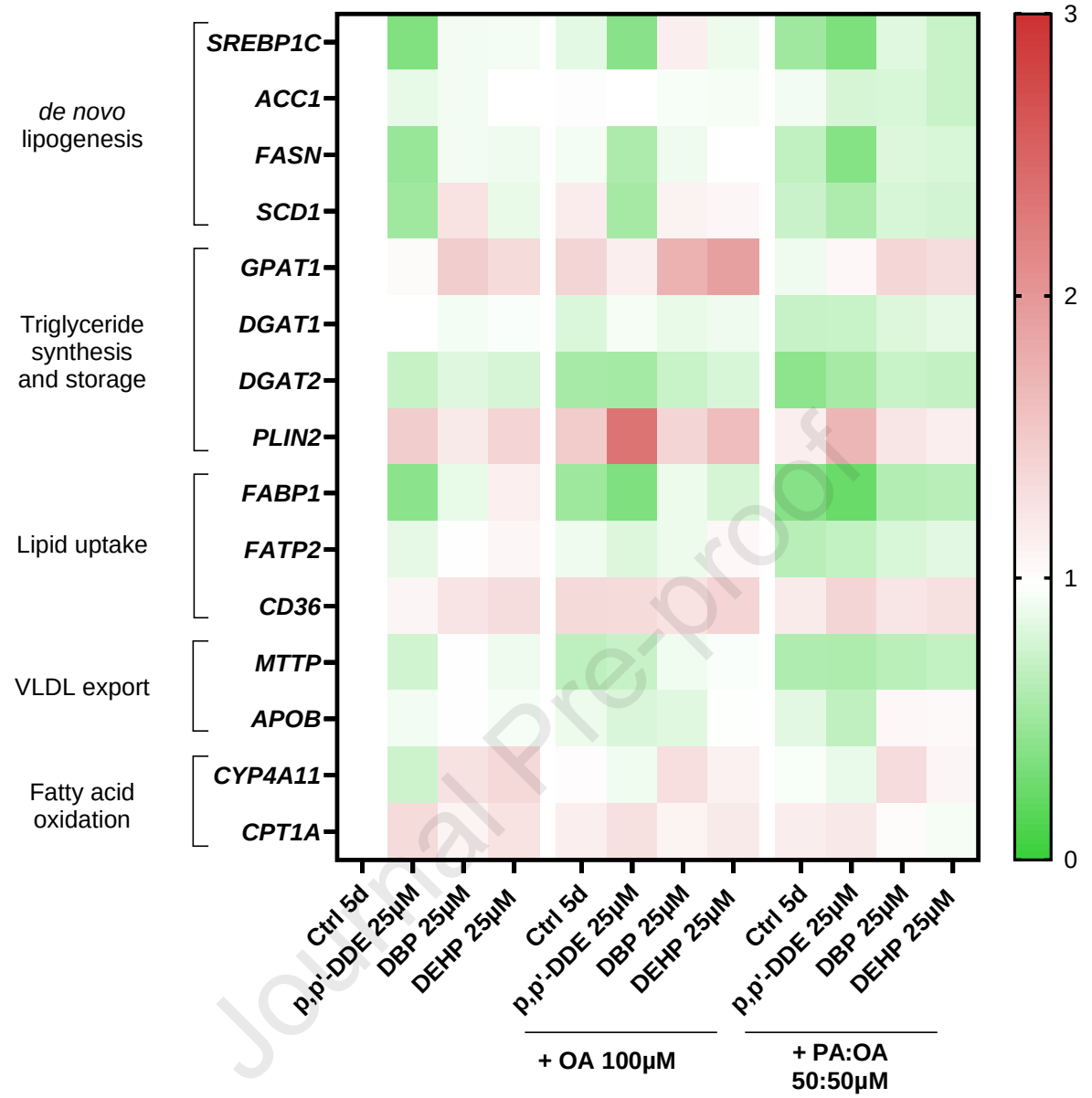

Figure 4: Heatmap of the impact of p,p'-DDE, DBP and DEHP exposure on lipid metabolism gene expression in 2D HepaRG cells. The mRNA levels of genes related to *de novo* lipogenesis, triglyceride synthesis and storage, lipid uptake, VLDL export and fatty acid oxidation were measured after 5 days of exposure to 25 µM EDCs alone or in combination with 100 µM oleic acid (OA) or a mixture of palmitic and oleic acid (PA:OA, 50:50 µM). The data are the means relative to the controls from at least 3 independent experiments. Statistical analysis was performed on treatments having the same supplementation conditions using one-way ANOVA followed by a Bonferroni correction or Kruskal-Wallis test followed by a Dunn's correction. Details of the qRT-PCR results for each gene are compiled in the **Supplementary Figures 5-9**.

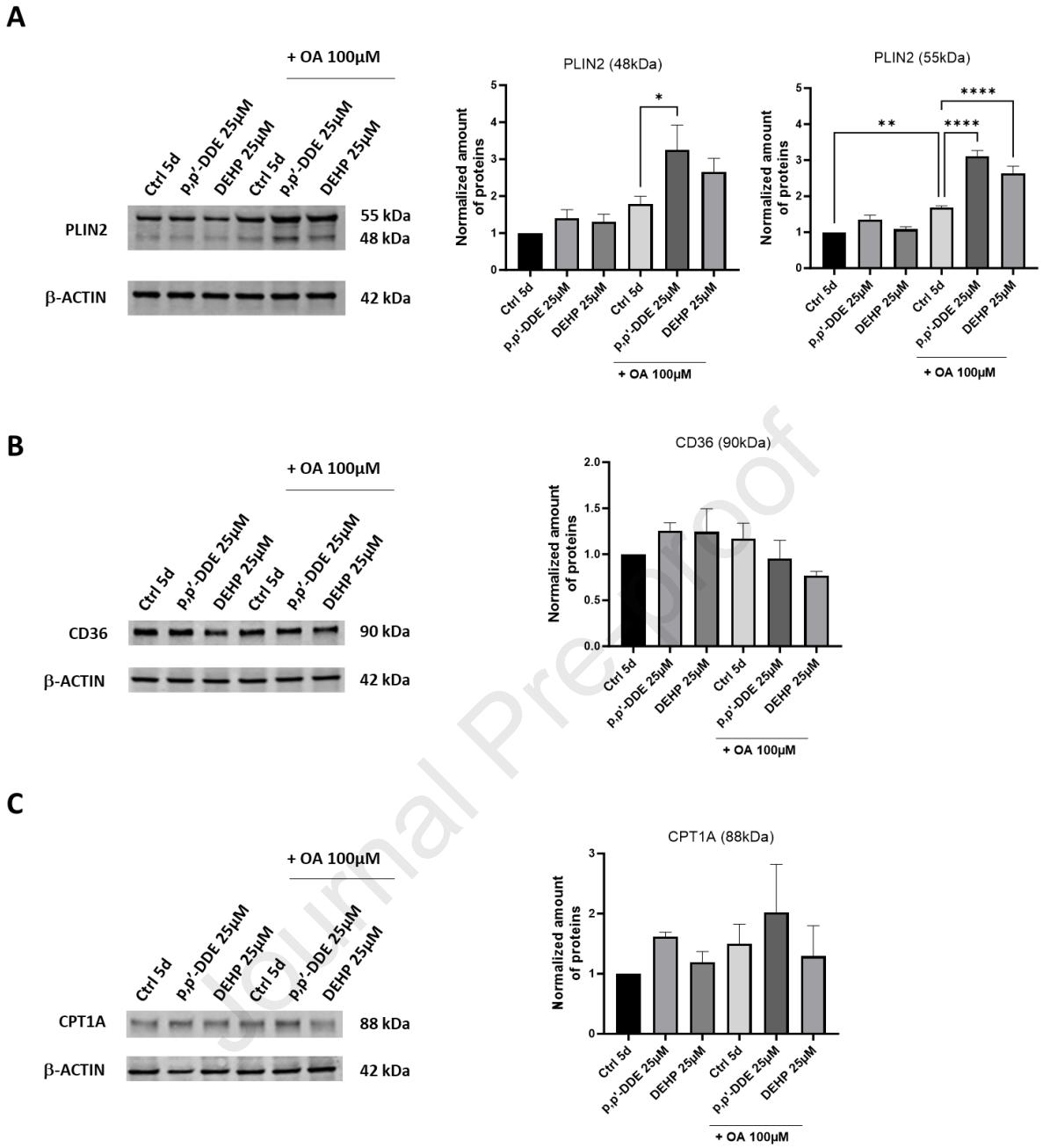

Figure 5: Impact of p,p'-DDE, DBP and DEHP exposure on lipid metabolism protein levels in 2D HepaRG cells. The levels of PLIN2 (**A**), CD36 (**B**) and CPT1A (**C**) expression were measured after 5 days of exposure to 25 µM p,p'-DDE or DEHP alone or with an 100 µM OA supplementation. Values are the mean ± SEM relative to the control from at least 3 (**B** and **C**) or 4 (**A**) independent experiments. Statistical analysis was performed on treatments having the same supplementation conditions using one-way ANOVA followed by a Bonferroni correction (**A**, **B** and **C**). *, $p < 0.05$; **, $p < 0.01$; ****, $p < 0.0001$.

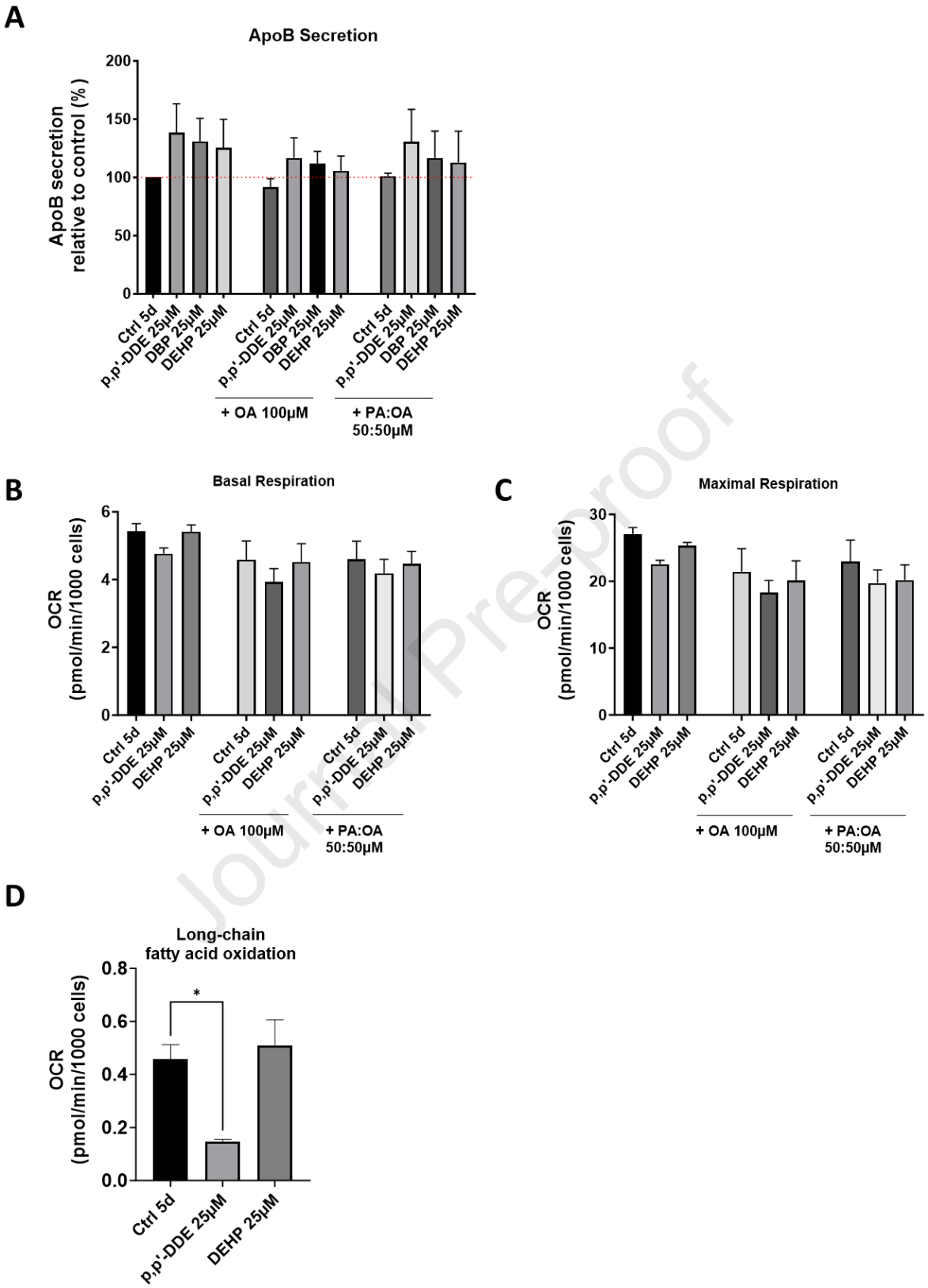

Figure 6: Impact of p,p'-DDE, DBP and DEHP exposure on physiological parameters related to lipid metabolism in 2D HepaRG cells. (**A**) The quantity of ApoB secreted was measured by ELISA after 5 days of exposure to 25 µM p,p'-DDE, DBP or DEHP alone or with

an OA (100 µM) or PA:OA (50:50 µM) supplementation. The medium was renewed after 2 days of exposure and the supernatants were collected 72h after the last treatment to assess the amount of ApoB. (**B** and **C**) The oxygen consumption rate (OCR) from mitochondrial respiration were measured after 5 days of exposure to 25 µM EDCs alone or in combination with 100 µM OA and a mixture of 50:50 µM PA:OA. The maximal respiration was calculated after FCCP injection. (**D**) The OCR relative to long-chain fatty acid oxidation (LCFAO) was determined after 5 days of exposure with 25 µM DDE and DEHP in HepaRG cells. The OCR from LCFAO was calculated as the difference between basal OCR and OCR after injection of 5 µM etomoxir (an inhibitor of CPT1A). Values are the means ± SEM from at least 3 (**B**, **C**, **D**) or 4 (**A**) independent experiments. Statistical analysis was performed on treatments having the same supplementation conditions using one-way ANOVA followed by a Bonferroni (**A**, **B**, **C**) or Dunnett (**D**) correction, *, $p < 0.05$.

Highlights

- DEHP induces the formation of lipid droplets in human HepaRG cells.
- Oleic acid (OA) supplementation enhances the steatotic effects of p,p'-DDE, DBP and DEHP.
- Perilipin 2 is overexpressed after co-exposure to OA and EDCs.
- p,p'-DDE exposure impairs long-chain fatty acid oxidation.
- A method developed for lipid droplet quantification could be used as a regulatory test.

Declaration of interests

☒ The authors declare that they have no known competing financial interests or personal relationships that could have appeared to influence the work reported in this paper.

☐ The authors declare the following financial interests/personal relationships which may be considered as potential competing interests: